International Journal of
Molecular Sciences

MDPI

Article

Deletion of Notch3 Impairs Contractility of Renal Resistance Vessels Due to Deficient Ca^{2+} Entry

Frank Helle [1,2], Michael Hultström [3,4,5,6,7], Panagiotis Kavvadas [1,2], Bjarne Iversen [3,4], Christos E. Chadjichristos [1,2] and Christos Chatziantoniou [1,2,*]

1 INSERM UMR S 1155, Hôpital Tenon, 75020 Paris, France
2 Faculty of Medicine, Sorbonne University, 75013 Paris, France
3 Renal Research Group, Institute of Medicine, University of Bergen, 5007 Bergen, Norway
4 Department of Medicine, Haukeland University Hospital, 5021 Bergen, Norway
5 Department of Biomedicine, University of Bergen, 5007 Bergen, Norway
6 Integrative Physiology, Department of Medical Cell Biology, Uppsala University, 75105 Uppsala, Sweden
7 Anaesthesiology and Intensive Care Medicine, Department of Surgical Sciences, Uppsala University, 75105 Uppsala, Sweden
* Correspondence: christos.chatziantoniou@sorbonne-universite.fr

Abstract: Notch3 plays an important role in the differentiation and development of vascular smooth muscle cells. Mice lacking Notch3 show deficient renal autoregulation. The aim of the study was to investigate the mechanisms involved in the Notch3-mediated control of renal vascular response. To this end, renal resistance vessels (afferent arterioles) were isolated from Notch3$^{-/-}$ and wild-type littermates (WT) and stimulated with angiotensin II (ANG II). Contractions and intracellular Ca^{2+} concentrations were blunted in Notch3$^{-/-}$ vessels. ANG II responses in precapillary muscle arterioles were similar between the WT and Notch3$^{-/-}$ mice, suggesting a focal action of Notch3 in renal vasculature. Abolishing stored Ca^{2+} with thapsigargin reduced Ca^{2+} responses in the renal vessels of the two strains, signifying intact intracellular Ca^{2+} mobilization in Notch3$^{-/-}$. EGTA (Ca^{2+} chelating agent), nifedipine (L-type channel-blocker), or mibefradil (T-type channel-blocker) strongly reduced contraction and Ca^{2+} responses in WT mice but had no effect in Notch3$^{-/-}$ mice, indicating defective Ca^{2+} entry. Notch3$^{-/-}$ vessels responded normally to KCl-induced depolarization, which activates L-type channels directly. Differential transcriptomic analysis showed a major down-regulation of *Cacna1h* gene expression, coding for the α_{1H} subunit of the T-type Ca^{2+} channel, in Notch3$^{-/-}$ vessels. In conclusion, renal resistance vessels from Notch3$^{-/-}$ mice display altered vascular reactivity to ANG II due to deficient Ca^{2+}-entry. Consequently, Notch3 is essential for proper excitation–contraction coupling and vascular-tone regulation in the kidney.

Keywords: Notch3; renal haemodynamics; Ca^{2+} mobilization; renal resistance vessels; vasoreactivity

Citation: Helle, F.; Hultström, M.; Kavvadas, P.; Iversen, B.; Chadjichristos, C.E.; Chatziantoniou, C. Deletion of Notch3 Impairs Contractility of Renal Resistance Vessels Due to Deficient Ca^{2+} Entry. *Int. J. Mol. Sci.* **2022**, *23*, 16068. https://doi.org/10.3390/ijms232416068

Academic Editor: Carolyn M. Ecelbarger

Received: 19 October 2022
Accepted: 13 December 2022
Published: 16 December 2022

1. Introduction

Notch is a family of membrane receptors participating in cell growth, differentiation, and apoptosis [1,2]. Out of the four isoforms (Notch1–4), the Notch3 receptor is specifically expressed in smooth vasculature [3] and has been shown to be crucial for the maturation of small arteries [4]. Notch3 expression seems to be functionally important only in certain vascular beds, such as in tail [5] and cerebral arteries [4], but not in the carotid artery [5] or skin [6].

In humans, a mutation in Notch3 causes the disorder cerebral autosomal-dominant arteriopathy with subcortical infarcts and leukoencephalopathy (CADASIL), which is an inherited small-vessel disease that causes ischemic strokes, mental disorders, and premature death [7,8]. In a genetic mouse model designed to mimic CADASIL, vascular smooth muscle cell degeneration was shown to precede the pathological changes [9,10],

suggesting that vascular dysregulation is likely to play a primary role in the pathogenesis of the disease.

The importance of renal vascular reactivity in controlling blood pressure led our group to study renal haemodynamics in mice lacking the Notch3 receptor [6]. Compared to wild-type littermates, Notch3$^{-/-}$ mice displayed a significantly blunted renal vascular response after systemic bolus injections of vasoactive agents, such as norepinephrine, angiotensin II (ANG II), bradykinin, or prostacyclin, consistent with deficient renal autoregulation. Furthermore, chronic infusion of ANG II was associated with increased mortality and severe renal damage in Notch3$^{-/-}$ mice [6]. These data indicate that Notch3 is essential for controlling renal vascular tone. However, in these previous studies, we did not elucidate the underlying cellular mechanism(s) involved in this dysfunction. In the present study, we investigated the contractile properties and Ca^{2+} responses of renal resistance vessels' freshly isolated afferent arterioles (AAs) from Notch3$^{-/-}$ mice.

Despite the expression of Ca^{2+} channels in many segments of the renal vascular tree [11], we focused on the AA because the afferent segment is of major importance when translating the ANG II signal to a vascular response [12] and is therefore most relevant for the changes observed in renal blood flow and renal vascular resistance in our earlier study [6]. Furthermore, defects of the afferent segment of the renal cortex are most compatible with nephropathy previously observed in some CADASIL patients [13,14].

Therefore, AAs isolated from Notch3$^{-/-}$ and wild-type mice were challenged with ANG II. The use of calcium channels or intracellular Ca^{2+} inhibitors indicated that the absence of Notch3 compromised entry of extracellular Ca^{2+}. The underlying mechanism of this defect was related to a significant downregulation of the α_{1H} subunit belonging to the T-type Ca^{2+} channel. It thus appears that Notch3 regulates renal vascular tone by controlling the expression and function of specific Ca^{2+} channels.

2. Results

2.1. Notch3 Deficiency Affects Vascular Contractility in a Tissue-Specific Manner

To test whether Notch3 affects vascular responses in a similar way in different tissues, we compared contractility responses to ANG II in a dose-dependent manner between abdominal muscle precapillary arterioles and AAs. Baseline diameters were similar in wild-type and Notch3$^{-/-}$ AAs (24.3 $\pm$ 2.1 µm vs. 24.2 $\pm$ 1.6 µm, respectively) and muscle resistance vessels (14.0 $\pm$ 2.1 vs. 14.0 $\pm$ 2.2 µm, respectively). As expected, the mean diameter of renal AAs isolated from wild-type mice decreased in a dose-dependent manner, reaching 60% of baseline at 10^{-7} M ANG II (Figure 1A). In contrast, renal vessels isolated from Notch3$^{-/-}$ mice showed little responsiveness to ANG II (barely a 10% decrease at 10^{-7} M ANG II, $p < 0.01$, Figure 1A). This strain difference was not observed when abdominal microvessels were challenged with the same doses of ANG II (60 $\pm$ 4% vs. 57 $\pm$ 7%, respectively, Figure 1B). These results suggest that the expression of Notch3 affects vessel contractility in a tissue-specific manner.

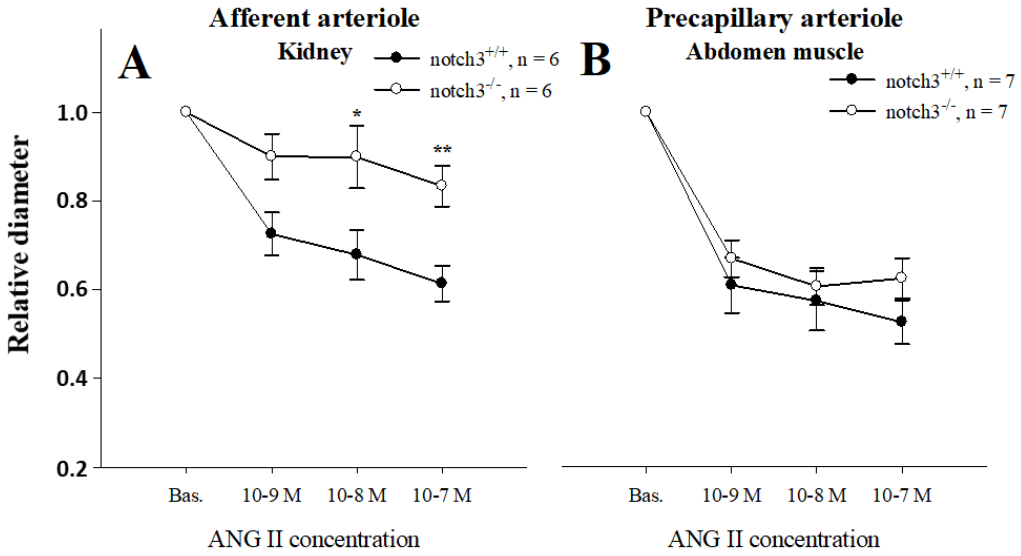

Figure 1. Lumen diameter dose-responses to angiotensin II (ANG II) in isolated afferent arterioles (AAs) revealed reduced contractile ability in renal vessels lacking Notch3 expression (**A**). In contrast, precapillary arterioles from abdominal muscle displayed similar contractions to ANG II (**B**). *, ** $p < 0.05$ and $p < 0.01$, respectively, vs. wild-type.

2.2. Notch3$^{-/-}$ Mice Display Decreased Levels of the T-Type Ca^{2+} Channel Subunit α_{1H} in the Renal Cortex

To elucidate the mechanism underlying the observed defective contractile response to acute administration of ANG II in AAs, we performed transcriptomic analysis on renal cortical slices from Notch3$^{-/-}$ and wild-type mice (Table A1). We focused on 47 genes well-known to control smooth muscle contractility. We found that the most striking difference between the two strains was the downregulation of Cacna1h, a gene coding the α_{1H} subunit of the T-type Ca^{2+} channel (Figure 2, Table A1).

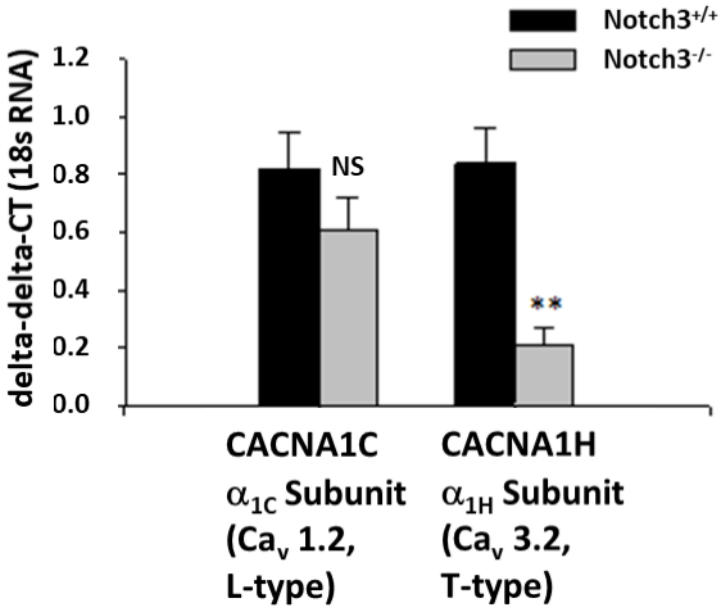

Figure 2. Expression of *Cacna1c* coding the α_{1C} subunit of the L-type Ca^{2+} channel did not statistically differ in renal cortex from kidneys of wild-type and Notch3$^{-/-}$ mice. In contrast, *Cacna1h* coding the α_{1H} subunit of the T-type Ca^{2+} channel was reduced 4-fold in Notch3$^{-/-}$ mice compared to wild-type mice (excerpt from Table A1, ** $p = 0.014$ vs. Notch$^{+/+}$).

2.3. Blunted Contractile Responses of AAs from Notch3$^{-/-}$ Mice Are Associated with Decreased Intracellular Ca^{2+} (Ca^{2+}_i) Levels

Renal vessels from Notch3$^{-/-}$ and wild-type mice displayed similar baseline values of Ca^{2+}_i (fura-2 ratio: 0.81 ± 0.03 vs. 0.83 ± 0.02, respectively). However, when vessels were challenged with ANG II, contraction and Ca^{2+}_i responses were weaker in AAs isolated from Notch3$^{-/-}$ kidneys ($p < 0.01$, Figure 3A,E). This result is consistent with the vessel diameter dose-responses shown in Figure 1.

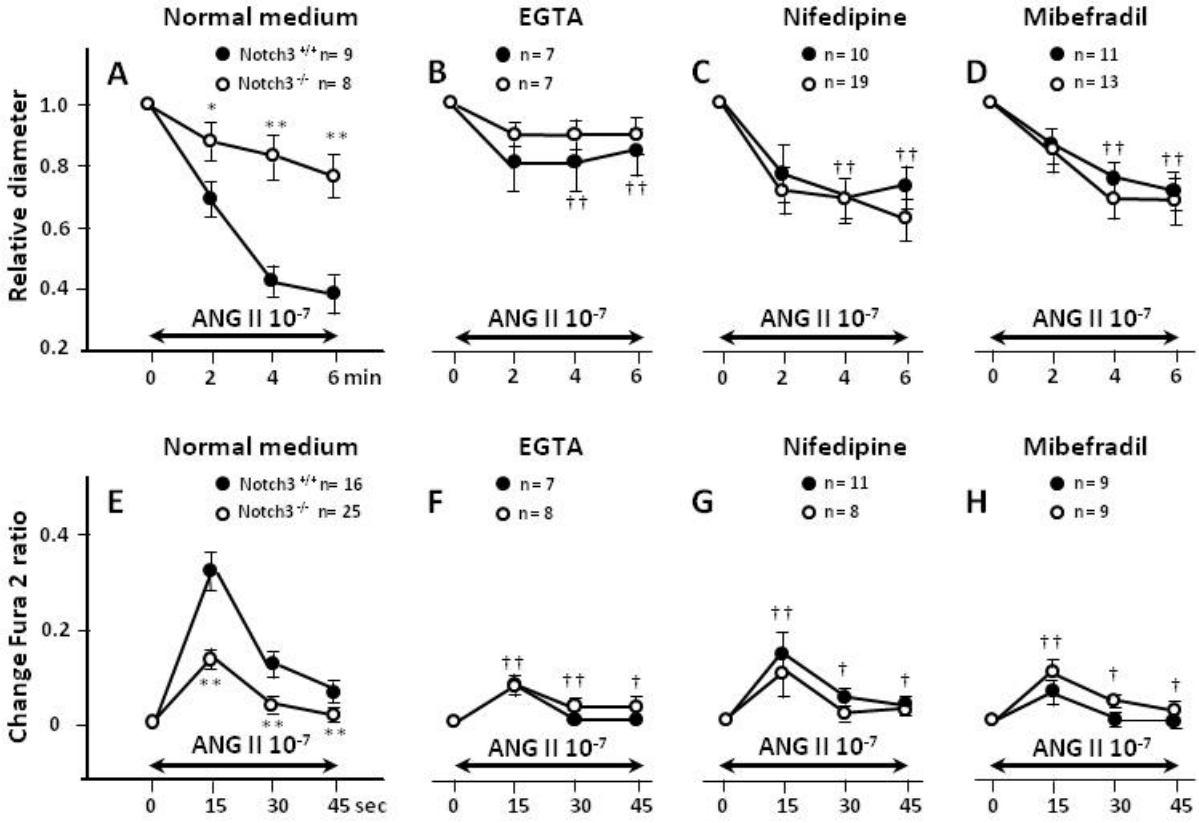

Figure 3. Changes in vessel diameter and Ca^{2+}_i responses to 10^{-7} M ANG II were measured in fura-2-loaded vessels freshly isolated from wild-type and Notch3$^{-/-}$ mice. In normal medium, both the diameter (**A**) and the Ca^{2+}_i response (**E**) were reduced in AAs lacking Notch3 expression. This strain difference in contractile and Ca^{2+}_i responses disappeared when Ca^{2+} was removed from the medium with EGTA (**B**,**F**), when L-type Ca^{2+} channels ($Ca_v1.2$) were blocked with nifedipine (**C**,**G**), or when T-type Ca^{2+} channels ($Ca_v3.2$) were blocked with mibefradil (**D**,**H**). It is noteworthy that the effect of these agents, which essentially target Ca^{2+} entry, is negligible on renal-resistant vessels from Notch3$^{-/-}$ mice. *, ** $p < 0.05$ and $p < 0.01$, respectively, vs. WT. †, †† $p < 0.05$ and $p < 0.01$, respectively, vs. corresponding response in normal medium.

2.4. Extracellular Entry of Ca^{2+} Is Compromised in AAs from Notch3$^{-/-}$ Mice

When Ca^{2+} was removed from the medium with EGTA, contractions and Ca^{2+} responses to ANG II were reduced in vessels from wild-type mice, but were unchanged in vessels from Notch3$^{-/-}$ mice (Figure 3B,F). As a result, the strain difference seen under basal conditions disappeared. Similarly, when Ca^{2+} was prevented from entering the cell through L- (Figure 3C,G) or T-type (Figure 3D,H) Ca^{2+} channels (inhibited with nifedipine and mibefradil, respectively), contractions were significantly blunted in vessels from wild-type mice. In contrast, the addition of these inhibitors did not affect the Ca^{2+} responses or contractility of Notch3$^{-/-}$ AAs. Again, the strain difference in the contractility and Ca^{2+} responses disappeared, suggesting that the reason for the improper response of the Notch3$^{-/-}$ vessels to ANG II was due to dysfunction in extracellular Ca^{2+} entry.

2.5. Intracellular Ca^{2+} Mobilization Is Normal in AAs from Notch3$^{-/-}$ Mice

To examine whether compromised $Ca^{2+}{}_i$ mobilization also contributed to blunted contractions, we treated AAs with the Ca^{2+} ATPase inhibitor thapsigargin, which abolishes intracellular calcium stores (Figure 4A,B). Thapsigargin treatment significantly reduced the peak Ca^{2+} response in both strains ($p < 0.001$), indicating that intracellular Ca^{2+} mobilization was equally efficient in the two strains.

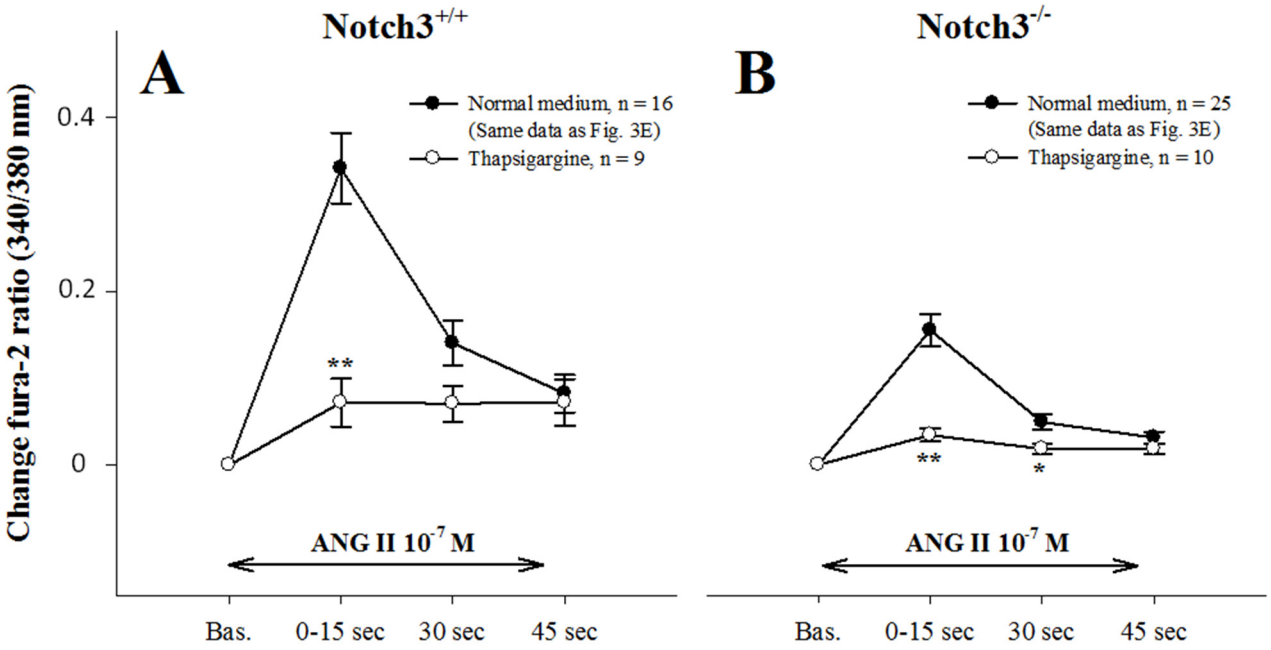

Figure 4. Ca^{2+} responses to 10^{-7} M ANG II, before and after administration of the Ca^{2+} ATPase inhibitor thapsigargin in wild-type (**A**) and Notch3$^{-/-}$ (**B**) vessels. Thapsigargin prevented Ca^{2+} mobilization from intracellular stores and reduced the peak Ca^{2+} response in both strains. * and ** $p < 0.05$ and $p < 0.001$, respectively, vs. corresponding response in normal medium.

2.6. AAs from Notch3$^{-/-}$ Mice Depolarize Normally

Since previous results indicated defects in calcium entry, we tested the function of L-type Ca^{2+}-entry in vessels from Notch3$^{-/-}$ mice using KCl-induced depolarization. Depolarization produced identical contractions and Ca^{2+} responses in both strains (Figure 5A,C), which were abolished by nifedipine blockade (Figure 5B,D).

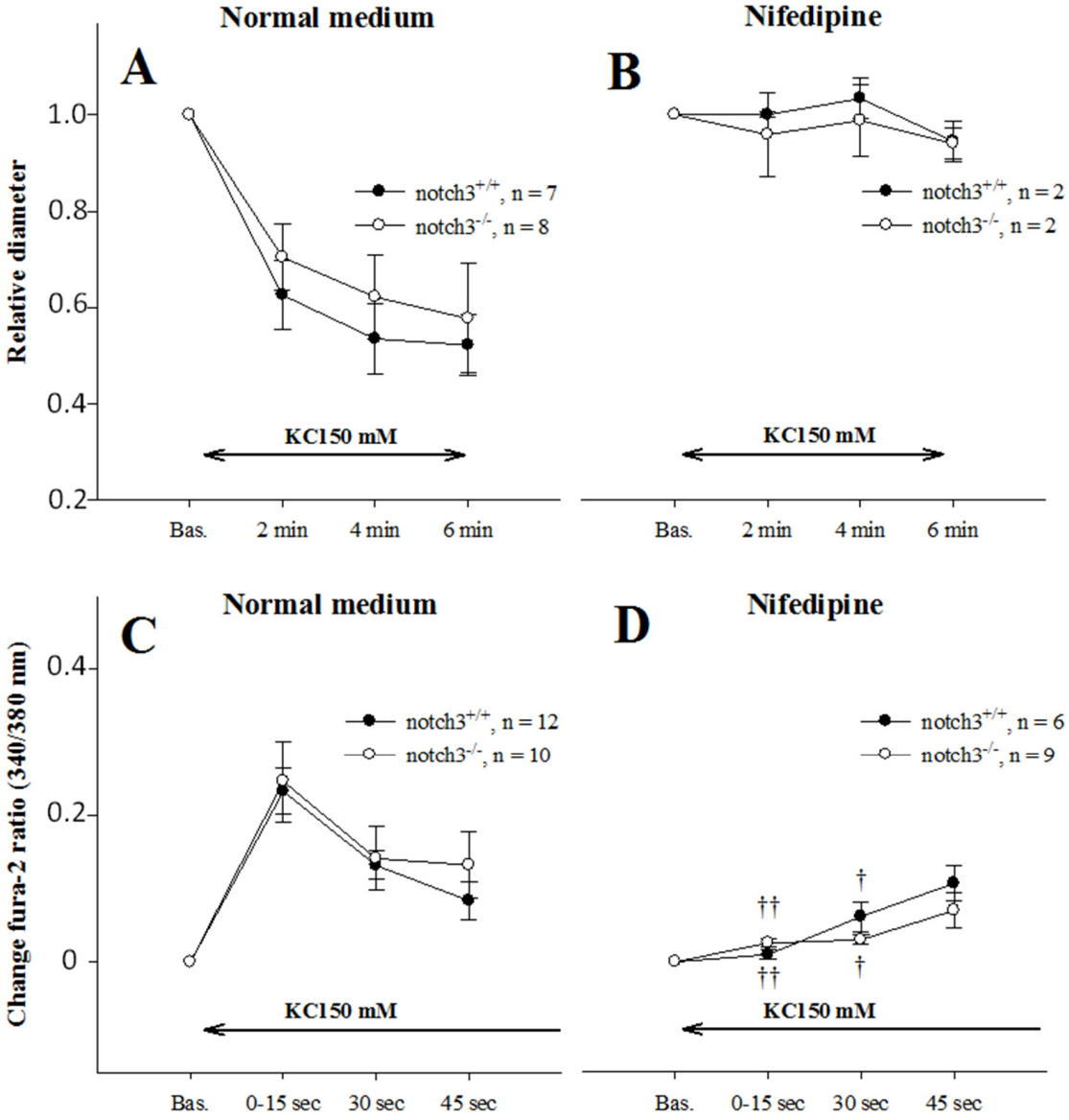

Figure 5. Diameter and Ca^{2+} responses after depolarization with 50 mM KCl in normal and fura-2-loaded afferent arterioles (AAs) from mice, with or without Notch3 expression. K^+ depolarization induced almost equal diameter (**A**) and Ca^{2+} responses (**C**) in the two strains. To test specificity, vessels were depolarized again with the L-type Ca^{2+} channel-blocker nifedipine in the bath. Results showed almost abolished diameter (**B**) and Ca^{2+} responses (**D**), confirming that the L-type Ca^{2+} channel was the active isoform in both strains, †, †† $p < 0.05$ and $p < 0.01$.

3. Discussion

Previous studies from our lab have shown that deletion of Notch3 in mice results in deficient in vivo renal responses to vasoactive agents. In the present study, our objective was to identify the mechanism(s) underlying the abnormal renal vascular response in mice lacking Notch3. To this end, we examined ANG II-induced contractility and $Ca^{2+}{}_i$ concentrations in renal resistance vessels isolated from Notch3$^{-/-}$ mice. We found that the renal vasculature of Notch3$^{-/-}$ mice does not respond normally to ANG II, possibly due to a deficient entry of Ca^{2+}.

Notch3$^{-/-}$ mice showed no differences in terms of body or kidney weight compared to wild-type littermates. Despite a thinner vessel wall of uneven thickness, as reported before in Notch3$^{-/-}$ [4,6], the two strains exhibited similar lumen diameter and baseline cytosolic Ca^{2+} concentrations. When challenged with ANG II, however, it was apparent that

contractions and Ca^{2+} responses to ANG II were much weaker in renal vessels of Notch3$^{-/-}$ mice (Figures 1A and 3A,E). It is important to note that the defective response was specific to renal vessels since pre-capillary vessels of other tissues responded normally (Figure 1B).

This defective response can be due to either impaired mobilization of $Ca^{2+}{}_i$ and/or Ca^{2+} entry. We tested the hypothesis of Ca^{2+} mobilization by using thapsigargin, a potent inhibitor of sarco/endoplasmic reticulum Ca^{2+}-ATPase. Thapsigargin addition in the medium completely blocked Ca^{2+} spikes in the afferent arterioles of WTs, as previously reported in vascular smooth muscle cells of resistance arteries [15]. An important decrease was also observed in afferent arterioles from Notch3$^{-/-}$ mice, suggesting that Ca^{2+} mobilization is not deregulated in the renal vessels of these mice. The fact that the observed decrease was bigger in the WTs' arterioles was due to higher levels of Ca^{2+} responses in a normal medium.

Removal of extracellular Ca^{2+} from the medium using EGTA strongly reduced contractility and Ca^{2+} concentration in normal renal vessels, in agreement with previous studies [16]. In sharp contrast, EGTA had a negligible effect on the responses of Notch3$^{-/-}$ vessels (Figure 3B,F). As result, the strain difference disappeared, and the contractility and Ca^{2+} concentrations became similar. These results strongly suggest that the defective response of Notch3$^{-/-}$ vessels is due to dysfunction of Ca^{2+} entry. Renal afferent arterioles display two types of Ca^{2+} channels: L-type and T-type [11]. Nifedipine, an L-type calcium blocker mimicked the effect of EGTA (reduced response in WT vessels, no effect in Notch3$^{-/-}$ vessels), suggesting dysfunctional L-type channels. However, the expression of L-type channels did not differ between the vessels of the Notch3$^{-/-}$ and WT (Table A1), and the results with KCl-induced depolarization (Figure 5) indicate that L-type channels are functioning correctly in Notch3$^{-/-}$.

The T-type Ca^{2+} channel is primarily expressed in preglomerular AAs [11]. Mibefradil, a T-type calcium blocker, also mimicked the effect of EGTA (reduced response in WT vessels; no effect in Notch3$^{-/-}$ vessels). In this case however, we observed a major decrease in the expression of the α_{1H} subunit of the T-type channel (*Cacna1h*) in Notch3$^{-/-}$ renal vessels (Table A1). In fact, *Cacna1h* was the most-affected gene compared to 46 other genes related to contractile function. We can thus hypothesize that the T-type Ca^{2+} channel is dependent on the Notch3 pathway for its expression on renal vessels. Alternatively, since a lack of Notch3 decreases smooth muscle actin expression and deforms the cytoskeleton and structure of the vascular wall (Table A1 [5,6,17]), it is possible that the expression of T-type Ca^{2+} on cell membranes was affected in Notch3$^{-/-}$ vessels. The low expression of this channel can explain, at least partly, the deficiency in the vascular response in the preglomerular vessels of Notch3$^{-/-}$ mice.

The question, however, remains: Why was Ca^{2+} entry from L-type channels also compromised? One possibility is that the decreased response of Notch3$^{-/-}$ afferent arterioles to ANG II is not due to a dysfunction of Ca^{2+} entry from its channels but is caused by an abnormality somewhere in the signalling from the ANG II receptor to the Ca^{2+} channels. This hypothesis is not supported by our previous study testing renal vascular responses in Notch3$^{-/-}$ mice [6]. In the previous study, we found deficient responses of Notch3$^{-/-}$ kidneys to other vasoconstrictors (such as norepinephrine or thromboxane) and to mechanical stress as well (which is independent of any kind of G-protein-receptor signalling pathway). This deficient response is extended to vasodilators, such as prostacyclin or bradykinin as well, showing that the deficient vasoconstriction is not due to a compensatory activation of a vasodilatory signalling.

Another hypothesis is that L- and T-type channels are interacting or cross-communicating, and a proper Ca^{2+} entry requires the appropriate functioning of both. The T-type channels are involved in excitability [18–21] and therefore impact the overall responsiveness of the vessel. Related to this role, it was reported that L- and T-type Ca^{2+} depend on each other to initiate contraction. In rabbit AAs, L-type Ca^{2+} entry is reliant on functional T-type Ca^{2+} channels [11]. Conversely, a blockade of the T-type Ca^{2+} channel has no effect on mice lacking the L-type channel [11]. In line with these findings, L- and T-type channel-

blockers have no additive effects on dilation in rat juxtaglomerular AAs, regardless of the order in which they are administered [22]. Using KCl depolarization and nifedipine, other investigators concluded that contractility and Ca^{+2} entry in afferent arterioles depend mainly on L-type channels with little contribution from T-type channels [23–25]. It is possible, however, that the low-current, transient T-type calcium flow happens but is unable to activate the high-conductance L-type channels because it cannot displace the nifedipine blockade. As a consequence, KCl-induced vasoconstriction is inhibited in the presence of nifedipine. Finally, it appears that that Ca^{2+} entry and mobilization in afferent arterioles make up a very complex mechanism involving interactions between L- or T- type, transient receptor potential, and K^+ and/or Cl^- channels as well [26]. It is possible that an interruption of this complex interplay at one step could affect the whole pathway of Ca^{2+} responses and contractility.

Alternatively, Ca^{2+} entry can be compromised in Notch3$^{-/-}$ renal vessels because the lack of the *Notch3* gene is accompanied by defects in vascular smooth muscle cell maturation [4,6]. Supporting this hypothesis, it was observed that Notch3-dependent postnatal arterial maturation did not correlate with the expression of the Notch3 ligands Jagged1 and Delta4 [4]. Instead, maturation of arterial vascular smooth muscle cells closely parallels the increase in arterial blood pressure during foetal development [27]. Based on these data, it was proposed that the transduction of pressure and shear stress from arteriolar blood flow to the vessel wall, necessary for arterial maturation of the actin cytoskeleton, is dependent on Notch3 signalling [4]. In agreement with this notion, we observed that the vascular wall of Notch3$^{-/-}$ afferent arterioles displayed an uneven thickness due to an incomplete maturation of vascular smooth muscle cells [6].

Whatever the nature of this interaction, our data show that the afferent arterioles of Notch3$^{-/-}$ mice depend mainly on intracellular $Ca^{2+}{}_i$ stores in order to respond to cardiovascular stress and vasoconstrictor stimuli. During control conditions, this appears to be adequate for maintaining vasoregulatory functions. During pathological conditions, however, such as those induced by prolonged exposure to exogenous ANG II [6], requiring extracellular $Ca2^+$ influx into the cells, mice lacking Notch3 fail to regulate renal haemodynamics, causing severe renal dysfunction and injury.

In our previous study of renal haemodynamics in Notch3$^{-/-}$ mice, we found a blunted and likely insufficient increase in RVR compared to wild-type ones after injecting 0.5 ng ANG II into the bloodstream. In contrast, blood pressure, indicating total peripheral resistance, increased equally in the two strains [6]. Consequently, while the kidney seems unable to generate a normal pressure response, the majority of resistance vessels in the Notch3$^{-/-}$ mouse must have a normal contractile response to ANG II. Consistent with this notion, we found a normal response to ANG II in muscle resistance vessels from Notch3$^{-/-}$, and we have previously obtained similar data from skin resistance vessels [6].

Other investigators found an almost passive increase in cerebral blood flow after ANG II injections in Notch3$^{-/-}$, but not wild-type, mice, while the blood pressure responses were similar [4]. Interestingly, another subunit of the T-type channel, α_{1G}, was shown to be downregulated several-fold in Notch3$^{-/-}$ cerebral vascular smooth muscle cells (SI Appendix Table 2A [28]). Taken together, these and our studies suggest that Notch3$^{-/-}$ vascular dysfunction in the brain and kidney may have molecular and cellular mechanistic similarities. Although different in some respects, the renal and cerebral vasculature share a vital physiological mechanism, the autoregulation of haemodynamics.

The list of genes in Table A1 shows that, in addition to *Cacna1h* (encoding the T-type Ca^{2+} channel), several genes affecting vessel contractility were also downregulated in the absence of Notch3. Examples from this list include connexin 43 (gap-junctions), transient receptor potential C6 (receptor-operated Ca^{2+} entry [29]), integrin-linked kinase (Ca^{2+}-independent contraction [30]), and rhoA (Notch3-dependent mechanotransduction [5]). Thus, it appears that additional signalling pathways controlling renal vasoreactivity are affected in Notch3$^{-/-}$ mice. The present finding of defective Ca^{2+} entry, however, is likely the foremost mechanism affecting the ANG II response in the renal preglomerular vessels.

We cannot exclude the possibility that other signalling pathways may have contributed to a lesser degree to this dysfunction, but if so, their impact was below what we can detect with the present model.

4. Materials and Methods

4.1. Animals

Experiments were performed on mice lacking expression of the *Notch3* gene (Notch3$^{-/-}$) on a C57Bl6/J background, as described elsewhere [6]. Wild-type littermates were used as controls. A total of 62 WT and Notch3$^{-/-}$ mice, weighing 18–25 g, were bred at the animal facility at the Institute of Biomedicine at the University of Bergen, fed ordinary mouse pellets, and had free access to tap water.

Because the objective of the study was to understand the deficient myogenic response in the kidney that we have observed previously [6], and since myogenic response depends on afferent and not on efferent arterioles, we isolated afferent arterioles from Notch3$^{-/-}$mice, and we compared them with afferent arterioles from their WT littermates. The analytical description for the isolation of preglomerular vessels, measurements of vessel diameters, and fura-2 intracellular Ca^{2+} ($Ca^{2+}{}_i$) responses to ANG II and KCl and chemicals are provided in the Appendix A.2.

4.2. Isolation of Preglomerular Vessels

Afferent preglomerular arterioles and precapillary muscle arterioles were isolated using an agarose-infusion/enzyme-treatment technique adapted from Loutzenhiser and Loutzenhiser [28]. In short, agarose-infused kidneys were sliced and digested with enzymes for 1 h. Free-floating intact vessels with a tensile core of agarose (Figure A1) were harvested and attached to a perfusion chamber before experiments.

4.3. Measurement of Vessels Diameter and $Ca^{2+}{}_i$ Responses

Isolated vessels were stimulated with ANG II (10^{-7} M or dose–response curves) or depolarised with KCl (50 mM) to study the Notch3 effects on contractility and Ca^{2+} transients, (see Appendix A.2). In short, mean diameter using digital image analysis and Ca^{2+} ratio using fura-2 340/380 nm emission was recorded at 37° C. AAs from both sexes were used after pilot studies showed no gender differences on contractility. Nifedipine (10^{-7} M), mibefradil (10^{-6} M), and thapsigargin (10^{-7} M) were applied to the vessel bath 15 min before the recordings.

4.4. mRNA Extraction and Expression Analysis Using RT-PCR

Slices of the renal cortex were stabilized in RNA-later (Qiagen, Valencia, CA, USA) and frozen until use. A quantity of 15–20 mg of tissue was used to prepare the total RNA using rNeasy (Qiagen, Valencia, CA, USA). RNA was quantified using a NanoDrop ND-1000 spectrophotometer (NanoDrop Technologies, Rockland, DE, USA). Reverse transcription was performed using the RT core-kit (Eurogentec, Seraing, Belgium) with 200 ng RNA. Real-time PCR was performed on an ABI-prism 7900-HT sequence-detection system at the Norwegian Microarray Consortium in Bergen using custom-made microfluidic cards: Taqman Low-Density Array (Applied Biosystems, Carlsbad, CA, USA). A total of 47 genes known to be involved in the contractile mechanism, Notch- or calcium-signalling, and 18s were selected for RT-PCR (Table A1). Gene expressions were calculated as delta-delta-CT using 18s RNA as standard with the RT-Manager program (Applied Biosystems, Carlsbad, CA, USA).

4.5. Statistical Methods

Vessel diameter and $Ca^{2+}{}_i$ responses with EGTA, nifedipine, and mibefradil vs. normal medium were analysed using ANOVA followed by the student–Newman–Keuls post hoc test in SigmaStat 3.1. Diameter and $Ca^{2+}{}_i$ responses in Notch3$^{-/-}$ vs. wild-type and thapsigargin $Ca^{2+}{}_i$ responses vs. normal medium were analysed using student's *t*-test in

SigmaStat 3.1. Gene expression was analysed using student's *t*-test and Bonferroni's correction. The genes were ordered after significance (Table A1), and the difference between the groups was expressed as Log2 fold-change (Log2FC). $p < 0.05$ was considered statistically significant. All values are expressed as means ± SEM.

5. Conclusions

The present study is, to our knowledge, the first to identify deficient Ca^{2+} entry as a major vasoactive signalling pathway dependent on Notch3 for proper function, which results in a serious defect of the calcium handling in the renal resistance vessels of mice lacking Notch3$^{-/-}$ expression. In AAs lacking Notch3, ANG II stimulation initiated Ca^{2+} mobilization, but that was not followed by Ca^{2+} entry. These data explain our previous observation that Notch3$^{-/-}$ kidneys are unable to cope with acute or prolonged ANG II infusion, and they also provide clues for the vascular function of Notch3 in other vascular beds, most notably the brain.

Author Contributions: Conceptualization: F.H., B.I., C.E.C. and C.C.; methodology: F.H., M.H. and P.K.; formal analysis F.H. and M.H.; writing—original draft preparation, F.H.; writing—review and editing, F.H., C.E.C. and C.C.; Visualization: F.H. and P.K. Resources: F.H. and C.C.; Project administration, C.C., B.I. and F.H. Funding acquisition: B.I., C.C. and F.H. All authors have read and agreed to the published version of the manuscript.

Funding: The study has been supported by grants from the Western Norway Regional Health Authority Fund and recurring, annual funding from Inserm and Sorbonne University. The supporters played no part in development or approval of the present manuscript.

Institutional Review Board Statement: All animal experiments were performed in strict accordance with good animal practices and animal research guidelines and were approved by the Norwegian State Board for Biological Experiments with Living Animals (07/80868 (#595)) and the appropriate committee of the Sorbonne University (Ref. No. B752001).

Informed Consent Statement: Not applicable.

Data Availability Statement: Not applicable.

Conflicts of Interest: The authors declare no conflict of interest. The funders had no role in the design of the study; in the collection, analyses, or interpretation of data; in the writing of the manuscript; or in the decision to publish the results.**Author Statement:** In memory of Bjarne Iversen, an outstanding man, clinician, mentor and researcher.

Appendix A

Appendix A.1. Isolation of Preglomerular Vessels

Afferent arterioles (AAs) (Figure A1A,B) and precapillary muscle arterioles (Figure A1C) were isolated from the renal cortex using the agarose-infusion/enzyme-treatment technique, adapted from Loutzenhiser and Loutzenhiser [31]. A quantity of 8 ml agarose-medium solution (20 mg/mL Seaprep, Cambrex, IA, USA, at 37 °C) was injected into the aorta (0.2 mL/s, excess fluid flushed out from vena cava incision) of anaesthetized mice (pentobarbital sodium 50–70 mg/kg). Kidneys and ~0.5 cm^3 muscle tissue were removed from the animals and incubated at 4 °C for 10 min for the solidification of the intraluminal agarose (Figure A1, arrowheads). Sections (cortical, if from kidneys) 100 µm thick were incubated at 37 °C for ~90 min (renal tissue) or ~100 min (muscle) in a medium enzyme-solution containing 0.5 mg/mL protease (Sigma P3417, 0.5 U/mL), 0.3 mg/mL collagenase (Sigma C5138, 700 U/mL), and 0.05 mg/mL trypsin inhibitor (Sigma T9003, to inhibit insidious clostripain contamination) in Roswell Park Memorial Institute (RPMI) medium without Ca^{2+}. Washing and gentle shaking produced free-floating, intact AAs completely free of connective tissue, identified positively by their relation to the glomerulus (kidney) or capillaries (muscle, Figure A1C, arrows) and the presence of intraluminal agarose. Vessels were harvested with a pressure-controlled pipette (tip diameter: 100–150 µm) and attached by self-adhesion to the surface of a clean No. 0 coverslip mounted in a Petri dish (MatTek

P35G-0-14-C) containing 3 mL medium. Each vessel was used for only one experiment. One or two arterioles were used from one animal for each experiment.

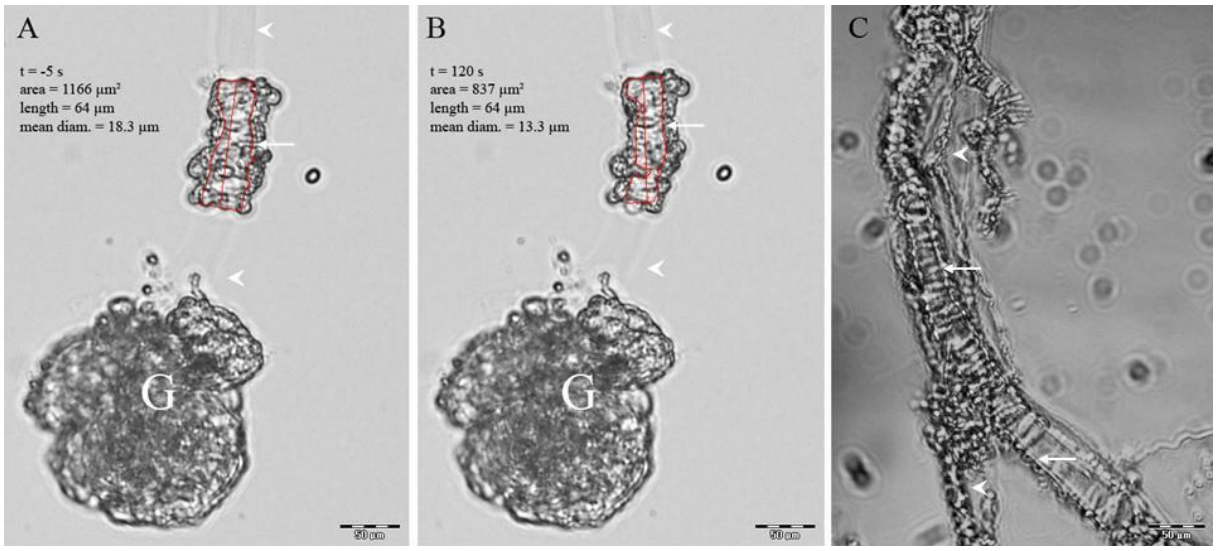

Figure A1. Representative tracing of wild-type afferent arteriole (AA) from mouse with intravascular agarose (arrow heads) isolated using the agarose-infusion/enzyme-treatment preparation (**A**,**B**). Red lines indicate the tracing of the lumen area and length, used to calculate mean lumen diameter. Identification was based on the relation to glomerulus (G). Precapillary resistance-arterioles from abdominal muscle also infused with agarose were identified based on branching capillaries (arrow heads) and had an easily identifiable vessel-wall lumen outline (arrows) used to trace diameters (**C**).

Appendix A.2. Diameter and Fura-2 Ca2+i Responses to ANG II and KCl

Vessels for calcium signalling studies were loaded using 15 µg/mL fura-2-AM ester for 60 min at room temperature, following 20 min of de-esterification at 37 °C. Using a perfusion-insert which reduced the volume of the Petri dish to 0.8 mL, vessels were perfused at 1–2 mL/s at 37 °C. The agonist protocol included either three successive ANG II doses (10^{-9}, 10^{-8} and 10^{-7} M) of 3 min duration (Figure A1), a single dose of ANG II 10^{-7} M (Figures 3 and 4), or 50 mM KCl (Figure 5) lasting either 6 min for diameter measurements or 150 s for $Ca^{2+}{}_i$ studies (see below).

Appendix A.3. Ca2+i Measurements

When applied, EGTA (2 mM), nifedipine (10^{-7} M), mibefradil (10^{-6} M), and thapsigargin (10^{-7} M) were added to both baseline and agonist perfusates, and the three latter preparations were incubated for an additional 15 min before the recordings. In the present experiments, we used a mibefradil concentration of 10^{-6} M, which is reported to ensure maximum effect [32]. Mibefradil has been shown to have nonspecific affinity to other ion-channels [33]. Such action is unlikely to have played a significant role in the present experiment since Notch3$^{-/-}$ AAs appeared resistant to the drug. For diameter measurements, pictures were acquired at baseline and at 2, 4, and 6 min after stimulation, using a ColorView IIIu on an inverted Olympus IX70 microscope (20× magnification, 1288 × 986 pixels, 0.34 µm/pixel). The area and length of the vessel-wall lumen were traced using Olympus DP-Soft 5.0 software and calculated as lumen area/lumen length (See Figure A1). For Ca^{2+} ratio measurements, the cells were excited alternatively with lights of 340 and 380 nm, using a dual-excitation wavelength system (Delta-Ram, PTI, USA). Then, 510 nm emission fluorescence images were recorded by an IC-200 intensified CCD camera and analysed using ImageMaster 5 software. Baseline was defined as the Ca^{2+} ratio 5 s before adding the agonist. The peak $Ca^{2+}{}_i$ response was calculated as the difference between the maximum Ca^{2+}-ratio between 0 s and 15 s after agonist stimula-

tion and baseline. The plateau responses at 30 s and 45 s after adding the agonist were calculated as the differences between the Ca^{2+}-ratios at these time points and baseline. If a Ca^{2+}-response stabilized at a value lower than the baseline, it was set to zero. The vascular preparation consisted of both smooth muscle and endothelium. The recorded Ca^{2+} ratios therefore represented the means of the two independent cytosolic compartments contained by these tissues, and we consequently reported data as Ca^{2+}-ratios rather than as absolute Ca^{2+} concentrations.

Appendix A.4. Chemicals-Reagents

All chemicals used in this experiment were obtained from Sigma, except fura-2-AM, which came from Molecular Probes. The RPMI media contained (in g/L) NaCl l 7.65, KCl 0.40, $MgCl_2$ 0.203, NaH_2PO_4 0.20, HEPES 1.34, glucose 1, 0 Na pyruvate 0.11, $CaHCO_3$ 0.35, $CaCl_2$ 0.22, RPMI vitamins (Sigma R7256), and amino acids (Sigma R7131).

Table A1. Comparative real-time PCR mRNA expression of 47 genes related to contractile function in the afferent arterioles from Notch3$^{-/-}$ and wild-type littermates. Note that the expression of *Cacna1h*coding the α_{1H} subunit of the T-type Ca^{2+} channel ($Ca_v3.2$) gene was strongly downregulated in Notch3$^{-/-}$ ($p < 0.001$ vs. wild-type). In contrast, *Cacna1c* coding the α_{1C} subunit of the L-type Ca^{2+} channel was similarly expressed in the two strains (No. 26 on the list).

No.	Gene	Symbol	ABI-Assay	WT (n = 11)	KO (n = 11)	Log2FC	*p*=
1	Notch-3	Notch-3	Notch3-Mm00435270_m1	1.55 ± 0.08	0.17 ± 0.16	−3.18	0.0000004
2	T-type Ca channel	Cacna1h	Cacna1h-Mm00445369_m1	0.84 ± 0.12	0.21 ± 0.06	−2.02	0.0003
3	Connexin 43	Gja1	Gja1-Mm00439105_m1	0.92 ± 0.13	0.51 ± 0.05	−0.85	0.009
4	smooth muscle actin	Acta2	Acta2-Mm00725412_s1	0.91 ± 0.12	0.54 ± 0.06	−0.75	0.01
5	MYPT1	Ppp1r12a	Ppp1r12a-Mm01234114_m1	0.60 ± 0.12	0.29 ± 0.04	−1.06	0.02
6	Transient receptor potential C6	Trpc6	Trpc6-Mm01176083_m1	1.27 ± 0.19	0.72 ± 0.11	−0.81	0.02
7	Hey2	Hey2	Hey2-Mm00469280_m1	0.76 ± 0.05	0.55 ± 0.07	−0.46	0.03
8	VE-cadherin	Cdh5	Cdh5-Mm00486938_m1	0.74 ± 0.05	0.6 ± 0.04	−0.3	0.03
9	rhoA	Rhoa	Rhoa-Mm00834507_g1	0.69 ± 0.03	0.62 ± 0.02	−0.15	0.04
10	Intergin-linked kinase	Ilk	Ilk-Mm00439671_g1	0.90 ± 0.05	0.73 ± 0.05	−0.3	0.04
11	IP3-receptor	Ip3r1	Itpr1-Mm00439917_m1	0.68 ± 0.02	0.62 ± 0.02	−0.12	0.05
12	PKC-alpha	prkca	Prkca-Mm00440858_m1	0.78 ± 0.03	0.68 ± 0.04	−0.2	0.05
13	calmodulin1	CaM	Calm1-Mm00486655_m1	0.64 ± 0.03	0.57 ± 0.02	−0.16	0.07
14	MLCP-catalytic subunit beta	Ppp1cb	Ppp1cb-Mm00554690_m1	0.30 ± 0.02	0.24 ± 0.03	−0.32	0.08
15	DMPK	dmpk	Dmpk-Mm00446261_m1	0.81 ± 0.08	0.63 ± 0.05	−0.35	0.08

Table A1. *Cont.*

No.	Gene	Symbol	ABI-Assay	WT (n = 11)	KO (n = 11)	Log2FC	*p*=
16	MLCK	Mylk	Mylk-Mm00653039_m1	0.72 ± 0.03	0.64 ± 0.04	−0.17	0.1
17	Cpi17	Ppp1r14a	Ppp1r14a-Mm00471820_m1	0.88 ± 0.08	0.72 ± 0.05	−0.29	0.11
18	ADP-ribosyl-cyclase	Cd38	Cd38-Mm00483146_m1	0.63 ± 0.03	0.56 ± 0.03	−0.18	0.13
19	Jag2	Jag2	Jag2-Mm00439935_m1	0.81 ± 0.06	0.68 ± 0.06	−0.26	0.14
20	ryanodine receptor 2	ryr2	Ryr2-Mm00465877_m1	1.13 ± 0.16	0.85 ± 0.1	−0.42	0.14
21	Connexin 37	Gja4	Gja4-Mm00433610_s1	0.85 ± 0.07	0.73 ± 0.05	−0.22	0.16
22	K^+ inw rect channel J11 ATPsens	Kcnj11	Kcnj11-Mm00440050_s1	1.21 ± 0.13	0.97 ± 0.11	−0.32	0.16
23	HeyL	HeyL	Heyl-Mm00516555_m1	0.79 ± 0.07	0.65 ± 0.07	−0.28	0.17
24	Tropomyosin 1	Tpm1	Tpm1-Mm00600378_m1	0.81 ± 0.09	0.67 ± 0.05	−0.28	0.17
25	ryanodine receptor 1	ryr1	Ryr1-Mm01175211_m1	1.35 ± 0.2	0.94 ± 0.21	−0.53	0.17
26	L-type Ca Channel	CACNA1C	Cacna1c-Mm00437917_m1	0.82 ± 0.13	0.61 ± 0.11	−0.42	0.26
27	Notch-4	Notch-4	Notch4-Mm00440536_g1	0.83 ± 0.05	0.77 ± 0.03	−0.11	0.3
28	Tbp	Tbp	Tbp-Mm00446973_m1	0.76 ± 0.02	0.72 ± 0.03	−0.07	0.31
29	Jag1	Jag1	Jag1-Mm00496902_m1	0.78 ± 0.06	0.7 ± 0.06	−0.17	0.32
30	connexin 40	GJA5	Gja5-Mm00433619_s1	0.66 ± 0.05	0.75 ± 0.08	0.19	0.33
31	Notch-1	Notch-1	Notch1-Mm00435245_m1	0.84 ± 0.06	0.77 ± 0.06	−0.12	0.39
32	Raf-1	Raf1	Raf1-Mm00466513_m1	0.85 ± 0.04	0.8 ± 0.05	−0.09	0.45
33	P/Q-type Ca channel	CACNA1A	Cacna1a-Mm00432190_m1	1.01 ± 0.1	0.91 ± 0.12	−0.16	0.49
34	DLL1	DLL1	Dll1-Mm01279265_g1	0.64 ± 0.08	0.58 ± 0.04	−0.14	0.55
35	Hey1	Hey1	Hey1-Mm00468865_m1	0.96 ± 0.1	1.05 ± 0.12	0.13	0.57
36	Ppia	Ppia	Ppia-Mm02342430_g1	0.79 ± 0.1	0.72 ± 0.08	−0.14	0.58
37	p38 MAPK	mapk14	Mapk14-Mm00442497_m1	0.68 ± 0.03	0.66 ± 0.03	−0.05	0.64
38	MLCP-catalytic subunit alpha	Ppp1ca	Ppp1ca-Mm00453295_g1	0.58 ± 0.01	0.57 ± 0.02	−0.03	0.69
39	Cacn2d2	Cacna2d2	Cacna2d2-Mm00457825_m1	1.55 ± 0.24	1.66 ± 0.17	0.1	0.7
40	MLCP-catalytic subunit gamma	Ppp1cc	Ppp1cc-Mm00849631_s1	0.84 ± 0.03	0.82 ± 0.04	−0.03	0.71

Table A1. *Cont.*

No.	Gene	Symbol	ABI-Assay	WT (n = 11)	KO (n = 11)	Log2FC	*p*=
41	Zip Kinase, Dap-like-kinase	Dapk3	Dapk3-Mm00492081_m1	0.69 ± 0.02	0.68 ± 0.03	−0.02	0.72
42	At1aR	Agtr1a	Agtr1a-Mm01166161_m1	0.65 ± 0.03	0.67 ± 0.04	0.03	0.76
43	Hes1	Hes1	Hes1-Mm00468601_m1	0.64 ± 0.05	0.62 ± 0.06	−0.04	0.82
44	Notch-2	Notch-2	Notch2-Mm00803077_m1	0.77 ± 0.05	0.78 ± 0.05	0.01	0.96
45	Pgk1	Pgk1	Pgk1-Mm00435617_m1	0.63 ± 0.02	0.63 ± 0.02	0	0.99
46	rho-k	Grk1	Grk1-Mm00442317_m1	Not Detected	Not Detected	0	NA
47	Hes5	Hes5	Hes5-Mm00439311_g1	Not Detected	Not Detected	0	NA

References

1. Iso, T.; Kedes, L.; Hamamori, Y. HES and HERP families: Multiple effectors of the Notch signaling pathway. *J. Cell. Physiol.* **2003**, *194*, 237–255. [CrossRef] [PubMed]
2. Schweisguth, F. Regulation of notch signaling activity. *Curr. Biol.* **2004**, *14*, R129–R138. [CrossRef] [PubMed]
3. Villa, N.; Walker, L.; Lindsell, C.E.; Gasson, J.; Iruela-Arispe, M.L.; Weinmaster, G. Vascular expression of Notch pathway receptors and ligands is restricted to arterial vessels. *Mech. Dev.* **2001**, *108*, 161–164. [CrossRef] [PubMed]
4. Domenga, V.; Fardoux, P.; Lacombe, P.; Monet, M.; Maciazek, J.; Krebs, L.T.; Klonjkowski, B.; Berrou, E.; Mericskay, M.; Li, Z.; et al. Notch3 is required for arterial identity and maturation of vascular smooth muscle cells. *Gen Dev.* **2004**, *18*, 2730–2735. [CrossRef]
5. Belin de Chantemele, E.J.; Retailleau, K.; Pinaud, F.; Vessieres, E.; Bocquet, A.; Guihot, A.L.; Lemaire, B.; Domenga, V.; Baufreton, C.; Loufrani, L.; et al. Notch3 is a major regulator of vascular tone in cerebral and tail resistance arteries. *Arterioscler. Thromb. Vasc. Biol.* **2008**, *28*, 2216–2224. [CrossRef]
6. Boulos, N.; Helle, F.; Dussaule, J.C.; Placier, S.; Milliez, P.; Djudjaj, S.; Guerrot, D.; Joutel, A.; Ronco, P.; Boffa, J.J.; et al. Notch3 is essential for regulation of the renal vascular tone. *Hypertension* **2011**, *57*, 1176–1182. [CrossRef]
7. Dichgans, M.; Mayer, M.; Uttner, I.; Bruning, R.; Muller-Hocker, J.; Rungger, G.; Ebke, M.; Klockgether, T.; Gasser, T. The phenotypic spectrum of CADASIL: Clinical findings in 102 cases. *Ann. Neurol.* **1998**, *44*, 731–739. [CrossRef]
8. Tournier-Lasserve, E.; Joutel, A.; Melki, J.; Weissenbach, J.; Lathrop, G.M.; Chabriat, H.; Mas, J.L.; Cabanis, E.A.; Baudrimont, M.; Maciazek, J.; et al. Cerebral autosomal dominant arteriopathy with subcortical infarcts and leukoencephalopathy maps to chromosome 19q12. *Nat. Gen.* **1993**, *3*, 256–259. [CrossRef]
9. Dubroca, C.; Lacombe, P.; Domenga, V.; Maciazek, J.; Levy, B.; Tournier-Lasserve, E.; Joutel, A.; Henrion, D. Impaired vascular mechanotransduction in a transgenic mouse model of CADASIL arteriopathy. *Stroke* **2005**, *36*, 113–117. [CrossRef]
10. Ruchoux, M.M.; Domenga, V.; Brulin, P.; Maciazek, J.; Limol, S.; Tournier-Lasserve, E.; Joutel, A. Transgenic mice expressing mutant Notch3 develop vascular alterations characteristic of cerebral autosomal dominant arteriopathy with subcortical infarcts and leukoencephalopathy. *Am. J. Pathol.* **2003**, *162*, 329–342. [CrossRef]
11. Hansen, P.B.; Jensen, B.L.; Andreasen, D.; Skott, O. Differential expression of T- and L-type voltage-dependent calcium channels in renal resistance vessels. *Circ. Res.* **2001**, *89*, 630–638. [CrossRef] [PubMed]
12. Navar, L.G.; Gilmore, J.P.; Joyner, W.L.; Steinhausen, M.; Edwards, R.M.; Casellas, D.; Carmines, P.K.; Zimmerhackl, L.B.; Yokota, S.D. Direct assessment of renal microcirculatory dynamics. *Fed. Proc.* **1986**, *45*, 2851–2861. [PubMed]
13. Guerrot, D.; Francois, A.; Boffa, J.J.; Boulos, N.; Hanoy, M.; Legallicier, B.; Triquenot-Bagan, A.; Guyant-Marechal, L.; Laquerriere, A.; Freguin-Bouilland, C.; et al. Nephroangiosclerosis in cerebral autosomal dominant arteriopathy with subcortical infarcts and leukoencephalopathy: Is NOTCH3 mutation the common culprit? *Am. J. Kidney Dis.* **2008**, *52*, 340–345. [CrossRef]
14. Kusaba, T.; Hatta, T.; Kimura, T.; Sonomura, K.; Tanda, S.; Kishimoto, N.; Kameyama, H.; Okigaki, M.; Mori, Y.; Ishigami, N.; et al. Renal involvement in cerebral autosomal dominant arteriopathy with subcortical infarcts and leukoencephalopathy (CADASIL). *Clin. Nephrol.* **2007**, *67*, 182–187. [CrossRef] [PubMed]
15. Fan, G.; Kaßmann, M.; Hashad, A.M.; Welsh, D.G.; Gollasch, M. Differential targeting and signaling of voltage-gated T-type Cav3.2 and L-type Cav1.2 channels to ryanodine receptors in mesenteric arteries. *J. Physiol.* **2018**, *596*, 4863–4877. [CrossRef] [PubMed]
16. Fellner, S.K.; Arendschorst, W.J. Voltage-gated Ca^{2+} entry and ryanodine receptor Ca^{2+}-induced Ca^{2+} release in preglomerular arterioles. *Am. J. Physiol. Ren. Physiol.* **2007**, *292*, F1568–F1572. [CrossRef] [PubMed]

17. Ghosh, S.; Paez-Cortez, J.R.; Boppidi, K.; Vasconcelos, M.; Roy, M.; Cardoso, W.; Ai, X.; Fine, A. Activation dynamics and signaling properties of Notch3 receptor in the developing pulmonary artery. *J. Biol. Chem.* **2011**, *286*, 22678–22687. [CrossRef]
18. Fellner, S.K.; Arendshorst, W.J. Angiotensin II Ca^{2+} signaling in rat afferent arterioles: Stimulation of cyclic ADP ribose and IP3 pathways. *Am. J. Physiol. Ren. Physiol.* **2005**, *288*, F785–F791. [CrossRef]
19. Hayashi, K.; Wakino, S.; Homma, K.; Sugano, N.; Saruta, T. Pathophysiological significance of T-type Ca^{2+} channels: Role of T-type Ca2+ channels in renal microcirculation. *J. Pharmacol. Sci.* **2005**, *99*, 221–227. [CrossRef]
20. Perez-Reyes, E. Molecular physiology of low-voltage-activated t-type calcium channels. *Physiol. Rev.* **2003**, *83*, 117–161. [CrossRef]
21. Moosmang, S.; Haider, N.; Bruderl, B.; Welling, A.; Hofmann, F. Antihypertensive effects of the putative T-type calcium channel antagonist mibefradil are mediated by the L-type calcium channel Cav1.2. *Circ. Res.* **2006**, *98*, 105–110. [CrossRef] [PubMed]
22. Feng, M.G.; Li, M.; Navar, L.G. T-type calcium channels in the regulation of afferent and efferent arterioles in rats. *Am. J. Physiol. Ren. Physiol.* **2004**, *286*, F331–F337. [CrossRef] [PubMed]
23. Vogel, P.A.; Yang, X.; Moss, N.G.; Arendshort, W.J. Superoxide enhances Ca^{2+} entry through L-type channels in the renal afferent arteriole. *Hypertension* **2015**, *66*, 374–381. [CrossRef] [PubMed]
24. Carmines, P.K.; Fowler, B.C.; Bell, P.D. Segmentally distinct effects of depolarization on intracellular [Ca^{2+}] in renal arterioles. *Am. J. Physiol. Ren. Physiol.* **1993**, *265*, F677–F685. [CrossRef] [PubMed]
25. Loutzenhiser, R.; Hayashi, K.; Epstein, M. Divergent effects of KCl-induced depolarization on afferent and efferent arterioles. *Am. J. Physiol. Ren. Physiol.* **1989**, *257*, F561–F564. [CrossRef]
26. Salomonsson, M.; Sorensen, C.M.; Arendshorst, W.J.; Steendahl, J.; Holstein-Rathlou, N.H. Calcium handling in afferent arterioles *Acta Physiol. Scand.* **2004**, *181*, 421–429.
27. Tiemann, K.; Weyer, D.; Djoufack, P.C.; Ghanem, A.; Lewalter, T.; Dreiner, U.; Meyer, R.; Grohe, C.; Fink, K.B. Increasing myocardial contraction and blood pressure in C57BL/6 mice during early postnatal development. *Am. J. Physiol. Heart Physiol.* **2003**, *284*, H464–H474. [CrossRef]
28. Arboleda-Velasquez, J.F.; Zhou, Z.; Shin, H.K.; Louvi, A.; Kim, H.H.; Savitz, S.I.; Liao, J.K.; Salomone, S.; Ayata, C.; Moskowitz, M.A.; et al. Linking Notch signaling to ischemic stroke. *Proc. Natl. Acad. Sci. USA* **2008**, *105*, 4856–4861. [CrossRef]
29. Fellner, S.K.; Arendshorst, W.J. Angiotensin II-stimulated Ca^{2+} entry mechanisms in afferent arterioles: Role of transient receptor potential canonical channels and reverse Na+/Ca^{2+} exchange. *Am. J. Physiol. Ren. Physiol.* **2008**, *294*, F212–F219. [CrossRef]
30. Wilson, D.P.; Sutherland, C.; Borman, M.A.; Deng, J.T.; Macdonald, J.A.; Walsh, M.P. Integrin-linked kinase is responsible for Ca^{2+}-independent myosin diphosphorylation and contraction of vascular smooth muscle. *Biochem. J.* **2005**, *392*, 641–648. [CrossRef]
31. Loutzenhiser, K.; Loutzenhiser, R. Angiotensin II-induced Ca^{2+} influx in renal afferent and efferent arterioles: Differing roles of voltage-gated and store-operated Ca^{2+} entry. *Circ. Res.* **2000**, *87*, 551–557. [CrossRef] [PubMed]
32. Cribbs, L.L. T-type Ca^{2+} channels in vascular smooth muscle: Multiple functions. *Cell Calcium* **2006**, *40*, 221–230. [CrossRef] [PubMed]
33. Jensen, L.J.; Holstein-Rathlou, N.H. Is there a role for T-type Ca^{2+} channels in regulation of vasomotor tone in mesenteric arterioles? *Can. J. Physiol. Pharmacol.* **2009**, *87*, 8–20. [CrossRef] [PubMed]